Theor Ecol (2015) 8:187–205
DOI 10.1007/s12080-014-0243-7

ORIGINAL PAPER

Homing fidelity and reproductive rate for migratory populations

Qihua Huang · Mark A. Lewis

Received: 16 July 2013 / Accepted: 19 November 2014 / Published online: 28 January 2015

Abstract Short-term and long-term population growth rates can differ considerably. While changes in growth rates can be driven by external factors, we consider another source for changes in growth rate. That is, changes are generated internally by gradual modification of population structure. Such a modification of population structure may take many generations, particularly when the populations are distributed spatially in heterogeneous environments. Here, the net reproductive rate R_0 is not sufficient to characterize short-term growth. Indeed, a population with net reproductive rate greater than one could initially decline precipitously, or a population with net reproductive rate less than one could initially grow substantially. Thus, we augment the net reproductive rate with lower and upper bounds for the transient reproductive rate, R_l and R_u. We apply these measures to the study of spatially structured salmon populations and show the effect of variable homing fidelity on short-term and long-term generational growth rates.

Keywords Homing fidelity · Net reproductive rate · Matrix models · Migration · Salmonidae · Transient growth rate

Q. Huang (✉) · M. A. Lewis
Centre for Mathematical Biology,
Department of Mathematical and Statistical
Sciences, University of Alberta, Edmonton,
AB, T6G 2G1, Canada
e-mail: qihua@ualberta.ca

M. A. Lewis
Department of Biological Sciences,
University of Alberta, Edmonton,
AB, T6G 2E9, Canada
e-mail: mark.lewis@ualberta.ca

Introduction

There is a growing recognition that short-term population dynamics can differ considerably from long-term asymptotic trajectories (Caswell and Neubert 2005; Ezard et al. 2010; Hastings 2001, 2004; Stott et al. 2011; Townley et al. 2007). Indeed, short-term declines may precede long-term asymptotic growth and, conversely, short-term growth may transit into long-term asymptotic declines (Koons et al. 2007; Neubert and Caswell 1997). Such transient dynamics may simply reflect changeable environmental conditions. However, they may also arise from an internal origin, that is, gradual changes in the population structure.

What form do gradual changes in population structure take? When there are stages, structured population theory (Caswell 2001; Cushing and Zhou 1994) tells us that the long-term asymptotic growth rate is achieved only when the population structure has achieved a corresponding stable stage distribution. This distribution may take many years to achieve, and when the distribution in stages differs from this stable stage distribution, the growth rate also differs. There may be more subtle changes in population structure at play if populations are distributed spatially. For example, a population that initially finds itself in poor quality habitat could decline and take many years before finding its way to high quality habitat where population growth is possible. It is this second eventuality of spatial structure affecting growth rates that we investigate in this paper.

The issue of population growth is of general interest in theoretical and conservation ecology. In many cases, population growth is calculated with matrix models. These are discrete-time age- or stage- structured population models that use demographic rates to project population dynamics (Caswell 2001). The population dynamics of matrix models can be analyzed with either the long-term population growth

rate λ_1 or the net reproductive rate R_0. The population growth rate λ_1 is given as the dominant eigenvalue of the projection matrix, and the associated stable stage distribution is given by the corresponding nonnegative right eigenvector. The net reproductive rate, R_0, is interpreted as the number of offspring produced by a *typical* individual over its lifetime (Caswell 2001). It is the dominant eigenvalue of the so-called next generation matrix, and the corresponding nonnegative right eigenvector represents the next generation stable stage distribution . Here, $\lambda_1 = 1$ if and only if $R_0 = 1$. The population grows when λ_1 or R_0 are greater than 1 and declines when λ_1 or R_0 are less than 1.

It is worth mentioning that the traditional method of calculating R_0 involves matrix operations that can be computationally complicated, particularly as the number of compartments in the models increases. Fortunately, a novel method to calculate and analyze R_0 directly from the life cycle graph of the matrix was developed in de-Camino-Beck and Lewis (2007), and with this method, it is straightforward to obtain an analytical formula for R_0. This is true even for complex life cycles, where the resulting expression can often be interpreted in terms of biologically relevant fecundity pathways. An fully algebraic counterpart of the graph reduction method was developed in Rueffler and Metz (2013), and various sets of sufficient and necessary conditions for R_0 to be a sum of contributions of fecundity pathways are given therein.

Most matrix population models do not consider spatial factors that affect population dynamics, and they typically assume a closed population, without dispersal or migration. This is unrealistic when individuals are found in subpopulations connected by dispersal or migration. This is particularly relevant when demography varies spatially among different habitats or subpopulations due to environmental heterogeneity. Hence, it may be necessary to classify individuals using geographical location as well as age or stage. Such spatial population models describe a finite set of discrete local populations, coupled by the movement of individuals. Such models are well documented in human demography where they are called *multiregional models* (Rogers 1968, 1995). In this paper, we refer to them as between-habitat patch models. A variety of scientific objectives motivate the development of these models, including investigating advantages gained by dispersal, critical numbers of patches for survival, the increase of species diversity in patchy environments, influence of dispersal upon evolutionary stable strategies, and the stabilizing influence of dispersal (Allen 1987; Deangelis et al. 1986; Ellner 1984; Gadgil 1971; Hamilton and May 1977; Horn and Macarthur 1972; Levin et al. 1984; Macarthur and Wilson 1967; Vance 1984).

Between-habitat patch models are particularly relevant to modeling migratory species. Migratory species usually travel a long distance from one place to another for reproduction or in search of new habitats. They may spend different life stages at different locations. Thus, migratory species need to be treated, not as single homogeneous population, but by explicitly including heterogeneity and connectivity over space.

The goal of this study is to understand how the interplay between connectivity and local population dynamics affects short-term and long-term growth rates for a migratory population in a network of heterogeneous patches. Our focus is on migratory populations. We use between-habitat patch models written in matrix form to describe the population dynamics of migratory species where the life cycle of the subpopulations is described explicitly in terms of stages, and the population connectivity is realized by the migrations of individuals between breeding and non-breeding areas. Here, the state variables are the number of individuals in each relevant stage class at each location. The key issue addressed by this study is how the strength of population connectivity, which is determined by homing fidelity during migration, affects the persistence of migratory species.

As an example, we consider the members of migratory *Salmonidae* family and examine the effect of migration on population persistence. The homing fidelity during migration in salmonids is variable (Stewart et al. 2004). Some migratory fish home with great fidelity while others show a high rate of straying. This motivates us to consider the important question: how does the degree of homing influence the population growth? We are interested in both long-term and short-term growth rates. The long-term growth rate is measured by the net reproductive rate R_0. The analysis of the dependence R_0 on the degree of homing fidelity indicates that in the long run, the overall population has a high net reproductive rate when most subpopulaitons show strong homing fidelity while a small fraction stray.

However, there is growing recognition that short-term, transient population dynamics can differ in important ways from long-term dynamics. For the short-term dynamics, we are interested in the growth rate over a single year or reproductive rate over a single generation. To understand the range in 1-year growth rates, we introduce two measures, λ_l and λ_u, that yield the lowest and highest possible yearly growth rates, respectively. We also consider dynamics over a single generation, a more relevant time scale for ecological considerations of species at risk of extinction or posing an invasion threat. We introduce two new measures of transient intergenerational growth, R_l and R_u, where R_l describes the lowest possible single generation population growth rates resulting from the initial distribution with all individuals in a poor quality patch, and R_u describes the highest single generation population growth rates resulting from the initial distribution with all individuals in a good quality patch.

The effect of homing fidelity on population growth is subtle. Its effect should depend upon whether individuals are initially in high quality or poor quality habitat. When individuals are in high quality habitat, homing fidelity will ensure that they remain in this good habitat, and thus can help maintain strong population growth. When individuals are in poor quality habitat, homing fidelity may prevent them from exploring and discovering the good quality habitat and can help to maintain weak population growth. To help understand these features mathematically, we investigate the influence of homing fidelity on R_0, R_l, and R_u. The quantity R_u depends on the homing fidelity in a similar way to R_0. That is, strong homing fidelity can increase R_u, yielding the highest possible single generation population growth rates as well as yielding a high net reproductive rate R_0. However, the relationship between R_l and the homing fidelity is opposite: homing fidelity can reduce R_l, reducing the lowest single generation population growth rates. Thus, while homing fidelity may increase the net reproductive rate, which is relevant to asymptotic time scales, it can reduce the reproductive rate on short time scales, particularly when the population is distributed spatially amongst good and poor quality patches in an unfavorable manner.

The rest of this introduction is organized as follows. First, we briefly introduce matrix models and show how to calculate R_0 using a graph reduction method. Then, we use a simple dispersal model to show the difference between asymptotic dynamics and transient dynamics in Section "A simple example: transient behavior versus asymptotic behavior". Finally, we introduce the life cycle of salmonidae as a focal example for demonstrating our approach.

Calculation of the net reproductive rate

Matrix models are widely used for demographic analysis of stage-structured population dynamics. A stage-structured matrix model is defined as

$$x(t+1) = \mathbf{P}x(t), \tag{1}$$

where $x(t) = [x_1(t), \cdots, x_n(t)]^T$ is a vector of stages at time t and $\mathbf{P}$ is an n by n nonnegative irreducible projection matrix describing transitions from one stage to another one (Caswell 2001). Matrix models can also be represented as a life cycle graph where each node in the graph corresponds to a stage and each arrow represents transitions from node to node (Fig. 1). The nonnegative matrix $\mathbf{P}$ is irreducible if its life cycle graph contains a path from every node to every other node. Biologically, this means that each stage is connected to all other ones, given enough time steps (Berman and Plemmons 1994; Ortega 1987).

One way to analyze the population dynamics of stage-structured matrix model is to calculate the net reproductive

$$\mathbf{P} = \begin{pmatrix} p_{11} & p_{12} \\ p_{21} & 0 \end{pmatrix}$$

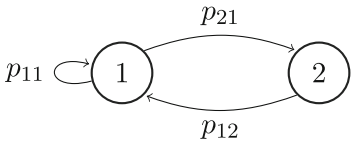

Fig. 1 A simple projection matrix and its associated graph. There is a directed edge in the graph for every nonzero entry p_{ij} in the matrix. For a transition, the edge is directed from node j to node i

rate, R_0, the average number of offspring produced by an individual over its lifetime (Caswell 2001). In order to calculate R_0, the projection matrix is decomposed as $\mathbf{P} = \mathbf{T} + \mathbf{F}$, where $\mathbf{T} = (\tau_{ij})$ contains the survivorship transitions and $\mathbf{F} = (f_{ij})$ the fecundities. Each entry in $\mathbf{T}$ describes the probability of an individual in stage j surviving to stage i in a single time step. This decomposition allows for the calculation of the net reproductive rate, R_0, defined mathematically as

$$R_0 = \rho\left(\mathbf{F}(\mathbf{I}-\mathbf{T})^{-1}\right), \tag{2}$$

where $\mathbf{I}$ is the identity matrix and $\rho(\cdot)$ denotes the spectral radius of the matrix $\mathbf{F}(\mathbf{I}-\mathbf{T})^{-1}$, which is referred to as the next generation matrix (Li and Schneider 2002). It has been shown (Cushing and Zhou 1994) that when $R_0 > 1$, the population grows, when $R_0 < 1$, the extinction state is stable, and when $R_0 = 1$, the extinction state is neutrally stable.

The calculation of R_0 using formula (2) is not always algebraically straightforward when there are many stages. First, the inverse of $\mathbf{I}-\mathbf{T}$ must be computed and then the eigenvalues of the next generation matrix must be calculated. However, a novel graph reduction method (de-Camino-Beck and Lewis 2007) provides a simple approach (see Appendix A).

The graph reduction method not only provides a straightforward approach for calculating net reproductive rate directly from the life cycle graph, but also yields an expression of R_0 as sum of contributions from the different possible fecundity pathways which is, biologically, a sequence of steps in the life cycle that lead to the production of new individuals (de-Camino-Beck and Lewis 2007). An example of the graph reduction method applied to a simple stage-structured model is shown in Fig. 11 in Appendix C.

A simple example: transient behavior versus asymptotic behavior

In this section, we use a simple migration model to show how short-term transient behavior of matrix models can be significant. The analysis then motivates us to introduce two measures that characterize the maximum and minimum transient growth rates.

We consider a population distributed in two discrete patches. We define $x_1(t)$ and $x_2(t)$ to be the size of subpopulations in these two patches in year t. Their growth rates are p_1 and p_2, respectively. We assume that $p_1 > 1 > p_2$ so one patch is a source and the other a sink. The migration rate of individuals from one patch to another is ϵ. We assume that ϵ is the same for both patches. We refer to the quantity ϵ as *connectivity* and the quantity $1-\epsilon$ as *homing fidelity*. The dynamics of this population are described by the model

$$\begin{pmatrix} x_1(t+1) \\ x_2(t+1) \end{pmatrix} = \begin{pmatrix} p_1(1-\epsilon) & p_2\epsilon \\ p_1\epsilon & p_2(1-\epsilon) \end{pmatrix} \begin{pmatrix} x_1(t) \\ x_2(t) \end{pmatrix}. \quad (3)$$

The growth rate of the overall population (denoted by λ_1), given as the dominant eigenvalue of the projection matrix (denoted by $\mathbf{P}$) in the model (3), can be calculated as the larger root of the quadratic equation:

$$\lambda_1^2 - (p_1+p_2)(1-\epsilon)\lambda_1 + p_1p_2(1-2\epsilon) = 0. \quad (4)$$

Clearly, the growth rate of overall population, λ_1, is a continuously differentiable function with respect to the migration rate ϵ. When $\epsilon = 0$, $\lambda_1 = \max\{p_1, p_2\}$, when $\epsilon = 1$, $\lambda_1 = \sqrt{p_1p_2}$. When $0 < \epsilon < 1$, the dependence of λ_1 on ϵ (left panel of Fig. 2) indicates that the population growth rate decreases as the migration rate increases.

The above eigenvalue analysis describes asymptotic growth rates and ignores short-term transient behavior, because the asymptotic growth rate (λ_1) is realized only when the population has reached so-called stable structure (given by the right eigenvector of $\mathbf{P}$ associated with λ_1). Natural questions arise: what happens before the asymptotic dynamics if the initial population distribution is not stable? how long it will take for the population to reach its asymptotic behavior? To answer these questions, as examples, we consider the solutions to the system (3) with initial distribution $[x_1(0), x_2(0)] = [0, 1]$ and connectivity either $\epsilon = 0.01$ or $\epsilon = 0.3$ (right panel of Fig. 2).

The asymptotic dynamics (left panel of Fig. 2) show that $\lambda_1(0.01) > \lambda_1(0.3) > 1$, which implies that the population will eventually grow exponentially for both values of ϵ, and the population will grow faster when $\epsilon = 0.01$ than it will when $\epsilon = 0.3$. However, as shown in the right panel of Fig. 2, the population initially declines for both values of ϵ, and the population level when $\epsilon = 0.3$ is actually higher than that when $\epsilon = 0.01$ for many years. This is because the local dynamics of the subpopulation in poor quality patch dominates the model dynamics for a long time, since the individuals are initially distributed in the poor quality patch and the connectivity strength ϵ is small.

Figure 2 highlights two key points: (1) short-term dynamics of system may be very different from long-term dynamics, and (2) transient behavior can be dramatic, long lasting, and counterintuitive. Therefore, the asymptotic growth rate λ_1 does not represent population dynamics in the short-term, and transient analysis of system is essential.

Motivated by the above example, we are concerned about short-term growth rate of a population whose dynamics are described by the model (1). In particular, we would like to find bounds for population growth rate. To this end, we define

$$\lambda_l = \min_{x(0)\geq 0, ||x(0)||_1=1} ||x(1)||_1, \quad (5)$$

as the minimum population growth in a single time step, where $||\cdot||_1$ is the ℓ_1 norm. It is straightforward to show that

$$\lambda_l = \min_{x\geq 0, ||x||_1=1} ||\mathbf{P}x||_1 = \min_{1\leq j\leq n} \sum_{i=1}^{n} p_{ij}, \quad (6)$$

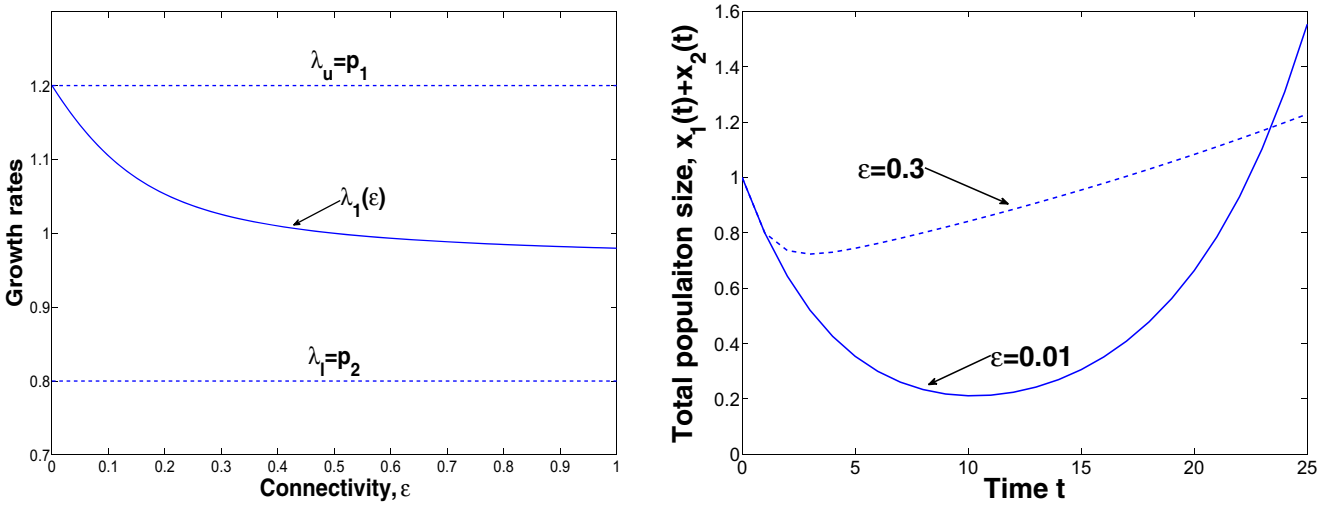

Fig. 2 (*Left*) The dependence of growth rate λ_1 on migration rate ϵ. (*Right*) The solutions of the model (3) with same initial distribution $[x_1(0), x_2(0)] = [0, 1]$ but different connectivity: either $\epsilon = 0.01$ *(solid line)* or $\epsilon = 0.3$ *(dashes line)*

the minimum sum of column vectors of projection matrix **P**. The proof is provided in the Appendix B.

Similarly, we define

$$\lambda_u = \max_{x\geq 0, ||x(0)||_1=1} ||x(1)||_1, \tag{7}$$

as the maximum population growth in a single time step. This is,

$$\lambda_u = \max_{x\geq 0, ||x||_1=1} ||\mathbf{P}x||_1 = \max_{1\leq j\leq n} \sum_{i=1}^{n} p_{ij}, \tag{8}$$

the maximum sum of column vectors of projection matrix **P**.

The quantities λ_l and λ_u bound the asymptotic growth rate λ_1:

$$\lambda_l \leq \lambda_1 \leq \lambda_u. \tag{9}$$

(Horn and Johnson 2013).

Applying the formulas (6) and (8) to the model (3), we find that $\lambda_l = \min\{p_1, p_2\}$ and $\lambda_u = \max\{p_1, p_2\}$, so they are independent of migration rate ϵ. For this reason, the two solution curves for different ϵ values (right panel of Fig. 2) have the same minimum one-step growth rate from $t = 0$ to $t = 1$, which is achieved when $[x_1(0), x_2(0)] = [0, 1]$.

Recently, Caswell and Neubert introduced a related set of indices into the ecological literature (Neubert and Caswell 1997) focusing on transient dynamics resulting from departure away a stable population structure, principal among these was "reactivity". Caswell and Neubert defined the reactivity (Caswell and Neubert 2005) as the maximum rate of departure from equilibrium $\hat{x} = 0$ immediately following a perturbation, i.e.,

$$\nu \equiv \log\left(\max_{||x(0)||_2=1} ||x(1)||_2\right), \tag{10}$$

where $||\cdot||_2$ is the ℓ_2 norm of vector. If $\nu > 0$, the equilibrium point is said to be "reactive". Actually, reactivity also gives the maximum growth rate from $t = 0$ to $t = 1$ as measured using the ℓ_2 norm.

Note that reactivity (10) uses ℓ_2 norm to describe the length of a vector in Euclidean space, which is the norm most amenable to mathematical manipulation (Neubert and Caswell 1997). However, it is not easy ascribe a biological meaning to the ℓ_2 norm. We employ ℓ_1 norm to measure the length of a vector in the definition of λ_u, since ℓ_1 norm is the sum of a non-negative vector with a clear interpretation as the total number of "individuals" across all stage classes. Also, we consider the geometric growth rate instead of arithmetic growth rate given in the definition of reactivity.

Two more new indices of transient dynamics that are related to next generation matrix are introduced in Section "Transient measures of generational population growth: R_l and R_u". Such indices are applicable to a generation time scale. By considering transient dynamics on a generational time scale, we gain two advantages: (1) a generational time scale is likely most relevant to endangered species, and (2) analysis on a generational time scale is much more amenable to algebraic calculations, because most next generation matrices are highly degenerated with low rank.

Salmonidae

Salmonidae is a family of ray-finned fish, including salmon, trout, char, freshwater whitefish, and grayling. Salmonids are native to the northern hemisphere, but have been introduced to many areas. There are currently 66 species recognized in this family, but the number of the species is actually greater than this (Salmonidae 2014). Salmonid species have experienced dramatic declines in abundance during the past several decades as a result of human and natural factors (Pacific Salmonids 2014).

Member of the salmonidae family share a very similar life cycle, following a series of stages as it develops from an egg to an adult fish. Most salmonid are migratory. Spawning always takes place in fresh water. During spawning, eggs are deposited by the female in an excavated nest on the substrate called a redd. Milt (sperm) is then deposited from the male fish to fertilize eggs. The fertilized eggs remain buried in the gravel and rocks of the stream bottom until about 1 month have passed. The fertilized eggs develop and hatch into alevin in the late winter or spring. Once it has absorbed its yolk, the alevin becomes a fry. Young fish are generally considered fry during their first year. Juvenile salmonids typically remain in fresh water for 1–3 years before they are ready to migrate downstream to large rivers, lakes, or oceans where they will spend the next phase of its life. When the fish have finished growing and attain sexual maturity, most species have a remarkable homing ability, typically returning to their natal streams to spawn even after having traveling hundreds of miles. Member of the salmonidae family can be either semelparous or iteroparous. Semelparous salmonids such as Pacific salmond die within a few days or weeks of spawning. Iteroparous salmonids such as Atlantic salmon and bull trout (*Salvelinus confluentus*) spawn more than once over their lifetimes.

We choose iteroparous salmonids as our study focus. In terms of the life history of iteroparous salmonids, we construct a stage-structured matrix model for resident species by dividing the population into four classes eggs: (E), fry (F), juveniles (J), and adults (A). Migratory salmonids spend different life stages at different locations. They make two types of migration in terms of their life cycle. The juvenile outmigration is from upstream freshwater rearing grounds to downstream large river or ocean; the adult upriver migration is from the large river or ocean back to the spawning grounds. We then formulate a two-patch

stage-structured model for migratory species, one patch represents the spawning area in upstream, and another patch represents the downstream habitat where the adults live. The variables in the two-patch model are eggs (E_1), fry (F_1), and juveniles (J_1) in patch 1 and juveniles (J_2) and adults (A_2) in patch 2. In this model, successful migration is an important factor that affects the population persistence. The two-patch migration model assumes that both upstream habitats and downstream habitats are spatially uniform, and that the population therefore has 100 % homing fidelity during migration. In reality, both upstream and downstream may contain many isolated local habitat due to environmental heterogeneity, this allows some individuals show a certain rate of straying during migration as observed. Therefore, to study how the interplay between homing fidelity and local population dynamics allows persistence in a network of heterogeneous patches, we extend the two-patch model to a four-patch interacting model by dividing the upstream spawning region into two patches and downstream into another two patches.

To address the question of homing influence on persistence, on the basis of four-patch interacting model, we introduce a connectivity constant ϵ to measure the homing degree of migratory fish, which also implies the strength of connectivity among subpopulations. We investigated the dependence of the overall population persistence on the strength of connectivity among subpopulations distributed at different locations and connected by migration.

This paper is organized as follows. In Section "R_0 for migratory salmonids", we develop a two-patch model for migratory salmonids and calculate R_0 for this population. We then extend the two-patch model to a four-patch interacting model. Based on the interacting model, we obtain a R_0 equation using the graph reduction method. We then study the effect of connectivity strength on R_0. In Section "The effect of homing fidelity on transient population persistence", we introduce new measures of transient population persistence, R_l and R_u. We then investigate the dependence of R_u and R_l on connectivity strength. Finally, a brief discussion section completes the paper.

R_0 for migratory salmonids

Matrix models provide an intuitive modeling strategy where the life cycle of the organisms can be described in terms of ages or stages. Salmonids may have either a resident or migratory life history. Resident species complete their entire life cycle in the same stream. Based on the life cycle of salmonids, we construct a stage-structured matrix population model for resident species and calculate the net reproductive rate R_0 for this population (see Appendix C).

Most salmonids are migratory. Two types of migration behavior are related to the migratory species: (1) Spawning migration takes place in breeding season. Adults move upstream to the spawning area after spawning, they return to the downstream, and (2) juvenile migration involves young fish. When young fish grows to juveniles, they leave the spawning area to reach downstream habitats of their parents. In this section, we first develop a two-patch model to describe the dynamics of migratory salmonids. The two-patch model is then extended to a four-patch interacting model due to spatial heterogeneity.

Model for migratory salmonids

To describe the dynamics of migratory salmonids, we denote the upstream and the downstream by patches 1 and 2, respectively. We define the population vector $N_i(t) = [E_i(t), F_i(t), J_i(t), A_i(t)]^T$ to be the density of the population at the end of the breeding season in year t at the patch i ($i = 1, 2$). We introduce notations, m_a, m_f, and m_j to represent the migration rates of adults, fry, and juveniles, respectively. More specifically, m_a represents the probability that adults living in the patch 2 in year t will appear at the patch 1 in year $t+1$ for reproduction, m_f is the probability that fry which live in the patch 1 in year t will appear at the patch 2 as juveniles in year $t+1$ due to growth and emigration, and m_j is the probability that juveniles located at patch 1 in year t will be found at the patch 2 in year $t+1$. We assume that all of spawning adults move back to patch 2 after breeding season ($A_1 = 0$) and that there are no eggs or fry in patch 2 ($E_2 = F_2 = 0$). The dynamics of migratory population can then be described by the following matrix model:

$$\begin{pmatrix} E_1(t+1) \\ F_1(t+1) \\ J_1(t+1) \\ J_2(t+1) \\ A_2(t+1) \end{pmatrix} = \begin{pmatrix} 0 & 0 & 0 & 0 & m_a b \\ p_{fe} & 0 & 0 & 0 & 0 \\ 0 & (1-m_f)p_{jf} & (1-m_j)p_{jj} & 0 & 0 \\ 0 & m_f p_{jf} & m_j p_{jj} & p_{jj} & 0 \\ 0 & 0 & 0 & p_{aj} & p_{aa} \end{pmatrix} \begin{pmatrix} E_1(t) \\ F_1(t) \\ J_1(t) \\ J_2(t) \\ A_2(t) \end{pmatrix}, \tag{11}$$

where the meanings of notations b, p_{fe}, p_{jf}, p_{jj}, p_{aj}, and p_{aa} are the same as those in the model (26) (Appendix C).

We calculate the net reproductive rate R_0 for the migratory salmonids using the graph reduction method. The calculation procedure is shown in Fig. 3 (see Appendix D for Fig. 12b–d). From the equation of R_0 (Fig. 3e), we see that the proportion of individuals that start as eggs in upstream, eventually survive to become breeding adults and migrate to downstream is given by

$$\frac{p_{fe}p_{aj}p_{jf}}{(1-p_{aa})(1-p_{jj})}\left(\frac{(1-m_f)m_j p_{jj}}{1-(1-m_j)p_{jj}} + m_f\right),$$

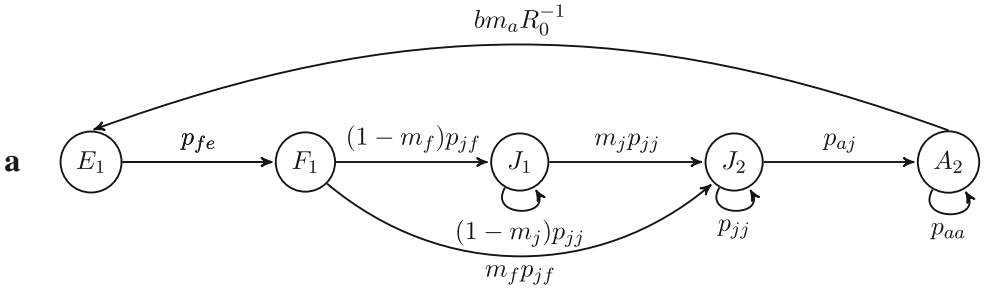

Fig. 3 **a** The full transformed graph. **e** Resulting net reproductive rate

e $$R_0 = \frac{bm_a p_{fe} p_{aj} p_{jf}}{(1-p_{aa})(1-p_{jj})}\left(\frac{(1-m_f)m_j p_{jj}}{1-(1-m_j)p_{jj}} + m_f\right)$$

the expected number of eggs produced per breeding adult is b, and the proportion of breeding adults that migrates from downstream to upstream during breeding season is m_a. Multiplying these quantities yields R_0.

Model for interacting migratory populations

It is widely believed that salmonids exist in environments composed of numerous ecological "islands" scattered over many local patches (Fraley and Shepard 1989; Underwood and Cramer 2007). This motivates us to extend the two-patch model to a multiple-patch model toward better understanding the dynamics of the population which is subdivided or patchy. For convenience, we extend the two-patch model to four-patch matrix model by dividing the upstream into two patches and downstream into another two patches. As we will see in the Discussion section, the four-patch model can be further extended to multiple-patch matrix model.

Model formulation and R_0

We assume that there are two small tributaries in upstream, denoted by patches 1 and 3, and two big streams in downstream, denoted by patches 2 and 4. Accordingly, the population vector $[E_i(t), F_i(t), J_i(t)]^T$ represents the density of the population in the patch i ($i = 1, 3$) in year t, and the population vector $[J_k(t), A_k(t)]^T$ is the density of the population in the patch k ($k = 2, 4$) in year t. We use the similar notations as those in models (26) (Appendix C) and Eq. 11 but assume that the population migration and survival rates depend on patches, hence m_a^{ik} represents the proportion that adults which live in the patch k in year t will appear at the patch i in year $t+1$, p_{jf}^{ki} is the proportion that fry which live in the patch i in year t will appear at the patch k in year $t+1$ as juveniles. Similar meanings for other notations. The four-patch interacting model is given by the following system of difference equations:

$$\begin{aligned}
E_1(t+1) &= b_1 m_a^{12} A_2(t) + b_1 m_a^{14} A_4(t)\\
F_1(t+1) &= p_{fe}^1 E_1(t)\\
J_1(t+1) &= \left(1 - m_f^{21} - m_f^{41}\right) p_{jf}^1 F_1(t)\\
&\quad + \left(1 - m_j^{21} - m_j^{41}\right) p_{jj}^1 J_1(t)\\
E_3(t+1) &= b_3 m_a^{32} A_2(t) + b_3 m_a^{34} A_4(t)\\
F_3(t+1) &= p_{fe}^3 E_3(t)\\
J_3(t+1) &= \left(1 - m_f^{23} - m_f^{43}\right) p_{jf}^3 F_3(t)\\
&\quad + \left(1 - m_j^{23} - m_j^{43}\right) p_{jj}^3 J_3(t)\\
J_2(t+1) &= m_f^{21} p_{jf}^{21} F_1(t) + m_j^{21} p_{jj}^{21} J_1(t)\\
&\quad + m_f^{23} p_{jf}^{23} F_3(t) + m_j^{23} p_{jj}^{23} J_3(t) + p_{jj}^2 J_2(t)\\
A_2(t+1) &= p_{aj}^2 J_2(t) + p_{aa}^2 A_2(t)\\
J_4(t+1) &= m_f^{41} p_{jf}^{41} F_1(t) + m_j^{41} p_{jj}^{41} J_1(t)\\
&\quad + m_f^{43} p_{jf}^{43} F_3(t) + m_j^{43} p_{jj}^{43} J_3(t) + p_{jj}^4 J_4(t)\\
A_4(t+1) &= p_{aj}^4 J_4(t) + p_{aa}^4 A_4(t). \qquad (12)
\end{aligned}$$

The procedure of calculating R_0 using graph reduction method is presented in Fig. 4 (see Appendix E for Fig. 13b–f).

Following the Fig. 4**d** (Appendix E), we set

$$g_{12} = \frac{p_{aj}^2 m_a^{12} b_1 p_{fe}^1}{1 - p_{aa}^2}, \quad g_{21} = \frac{m_f^{21} p_{jf}^{21}}{1 - p_{jj}^2} + \frac{\left(1 - m_f^1\right) p_{jf}^1 m_j^{21} p_{jj}^{21}}{\left[1 - (1 - m_j^1) p_{jj}^1\right]\left(1 - p_{jj}^2\right)},$$

$$g_{14} = \frac{p_{aj}^4 m_a^{14} b_1 p_{fe}^1}{1 - p_{aa}^4}, \quad g_{41} = \frac{m_f^{41} p_{jf}^{41}}{1 - p_{jj}^4} + \frac{\left(1 - m_f^1\right) p_{jf}^1 m_j^{41} p_{jj}^{41}}{\left[1 - (1 - m_j^1) p_{jj}^1\right]\left(1 - p_{jj}^4\right)},$$

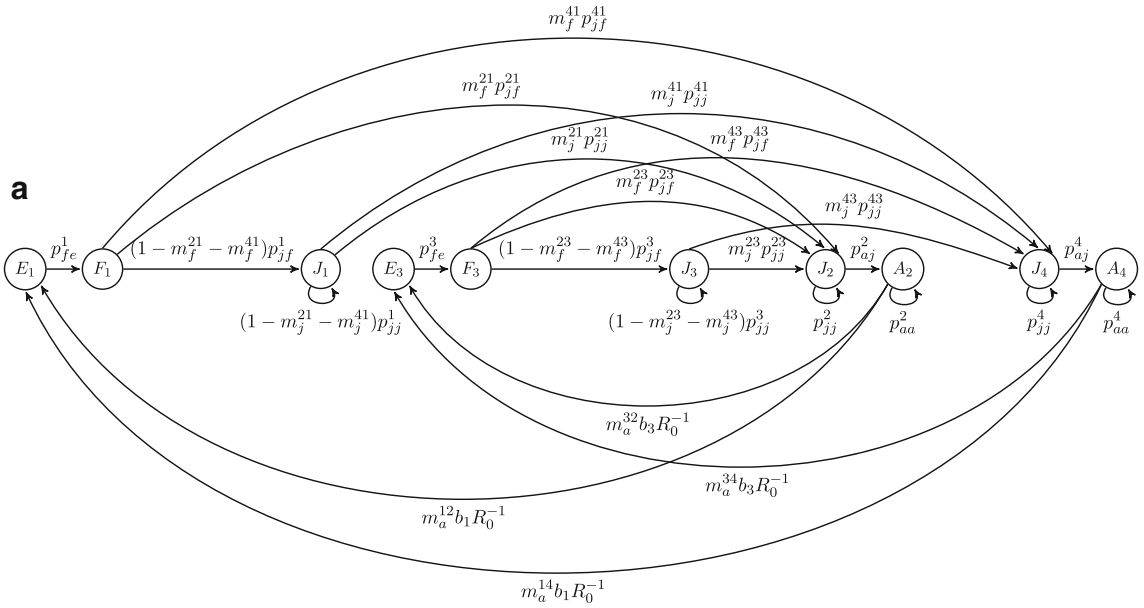

Fig. 4 **a** The full transformed graph

$$g_{32} = \frac{p^2_{aj} m^{32}_a b_3 p^3_{fe}}{1-p^2_{aa}}, \quad g_{23} = \frac{m^{23}_f p^{23}_{jf}}{1-p^2_{jj}} + \frac{\left(1-m^3_f\right) p^3_{jf} m^{23}_j p^{23}_{jj}}{\left[1-(1-m^3_j)p^3_{jj}\right]\left(1-p^2_{jj}\right)},$$

$$g_{34} = \frac{p^4_{aj} m^{34}_a b_3 p^3_{fe}}{1-p^4_{aa}}, \quad g_{43} = \frac{m^{43}_f p^{43}_{jf}}{1-p^4_{jj}} + \frac{\left(1-m^3_f\right) p^3_{jf} m^{43}_j p^{43}_{jj}}{\left[1-(1-m^3_j)p^3_{jj}\right]\left(1-p^4_{jj}\right)}, \tag{13}$$

where m^1_f represents the proportion that fry living in the patch 1 in year t will appear in the downstream as juveniles for further growth, that is, $m^1_f = m^{21}_f + m^{41}_f$. Similar meaning for the notations m^1_j, m^3_f, and m^3_j. Then, from the Fig. 4; **f** (Appendix E), R_0 can be calculated as the larger root of the following quadratic:

$$\begin{aligned} R_0^2 &- (g_{21}g_{12} + g_{41}g_{14} + g_{23}g_{32} + g_{43}g_{34})R_0 \\ &- g_{21}g_{32}g_{43}g_{14} - g_{41}g_{34}g_{23}g_{12} \\ &+ g_{21}g_{12}g_{43}g_{34} + g_{41}g_{14}g_{32}g_{23} = 0. \end{aligned} \tag{14}$$

It is easy to find that the discriminant of the quadratic (14) is positive; hence, the Eq. 14 has two real roots. If all spawners home with 100 % fidelity when they migrate, for instance, all spawners living in patch 2 always show fidelity to their natal tributary stream, say patch 1, and all fry and juveniles living in patch 1 emigrate to the patch 2, the habitat of their parents, and similar homing behavior for the subpopulation living in patches 3 and 4, then the four-patch model reduces to two disjoint two-patch models. Since there is no interaction between patch 1 and 4 or between patch 2 and 3, letting $g_{14} = g_{41} = g_{32} = g_{23} = 0$ in Eq. 13, we obtain the net reproductive rates $R_0^{12} = g_{12}g_{21}$ for the subpopulation living in patches 1 and 2, and $R_0^{34} = g_{34}g_{43}$ for the subpopulation living in patches 3 and 4, which are consistent with the R_0 expression **e** in Fig. 3, resulting from the two-patch model (11).

However, salmonids do not always exhibit strong homing fidelity: the homing ability of salmonids appears to be variable and is perhaps an adaptive trait that is subject to natural selection (McPhail and Baxter 1996; Stewart et al. 2004). The degree of homing maybe related to stream size and stability (McPhail and Baxter 1996). Since the connectivity strength is realized through migration rates, a diagram which describes the interactions is presented in Fig. 5.

From Fig. 5, when $0 < \epsilon \ll 1$, most migrations take place between patch 1 and patch 2 and between patch 3 and patch 4, very few migrations take place between patch 1 and patch 3 or between patch 2 and patch 4. For this case, we think of the migration routes between patch 1 and patch 2 and between patch 3 and patch 4 as *homing routes*, and the migration routes between patch 1 and patch 4 and between patch 3 and patch 2 as *straying routes*. Thus, when ϵ is close to 1, the above-mentioned homing routes become straying routes and straying routes become homing routes. When $\epsilon = 0$ or $\epsilon = 1$, only homing routes exist. Finally, when $\epsilon = 1$, there is no connection between patch 1 and patch 2 or between patch 3 and patch 4. The relevant net reproductive rates for the two disjoint two-patch models are $R_0^{14} = g_{14}g_{41}$ and $R_0^{32} = g_{32}g_{23}$.

Clearly, if two patches (patches 1 and 3) in upstream are equal in their quality and two patches (patches 2 and 4) in downstream are equal as well, then homing versus straying

would make no difference, in this case, the degree of homing fidelity does not play a role on the reproductive rate. In our study, we always assume that the patches are unequal in their quality.

The effect of connectivity strength ϵ on R_0

In what follows, we use the R_0 equation (14) to investigate the effect of connectivity strength on R_0. Following Fig. 5, we rewrite g_{12}, g_{14}, and g_{21} given in Eq. 13 as

$$\begin{aligned} g_{12} &= \frac{(1-\epsilon)m_a^2 p_{aj}^2 b_1 p_{fe}^1}{1-p_{aa}^2} =: (1-\epsilon)G_{12}, \\ g_{14} &= \frac{\epsilon m_a^4 p_{aj}^4 b_1 p_{fe}^1}{1-p_{aa}^4} =: \epsilon G_{14} \\ g_{21} &= \frac{(1-\epsilon)m_f^1 p_{jf}^{21}}{1-p_{jj}^2} + \frac{\left(1-m_f^1\right) p_{jf}^1 (1-\epsilon) m_j^1 p_{jj}^{21}}{[1-(1-m_j^1)p_{jj}^1]\left(1-p_{jj}^2\right)} \\ &:= (1-\epsilon)G_{21}, \end{aligned}$$

Similarly, we can write

$$g_{41} = \epsilon G_{41}, \quad g_{32} = \epsilon G_{32}, \quad g_{23} = \epsilon G_{23},$$

$$g_{43} = (1-\epsilon)G_{43}, \quad g_{34} = (1-\epsilon)G_{34}.$$

Thus, from the R_0 equation (14), we have R_0 as the larger root of the quadratic:

$$R_0^2 - \left[A(1-\epsilon)^2 + B\epsilon^2\right] R_0 - C\epsilon^2(1-\epsilon)^2 + D\epsilon^4 + E(1-\epsilon)^4 = 0, \tag{15}$$

where

$$\begin{aligned} A &= G_{21}G_{12} + G_{43}G_{34}, \quad B = G_{41}G_{14} + G_{23}G_{32}, \\ C &= G_{21}G_{32}G_{43}G_{14} + G_{41}G_{34}G_{23}G_{12}, \\ D &= G_{41}G_{14}G_{23}G_{32}, \\ E &= G_{21}G_{12}G_{43}G_{34}. \end{aligned}$$

When $\epsilon = 0$ or $\epsilon = 1$, the system is reducible and is decoupled into two subsystems, each of which has a different R_0. R_0 can no longer be defined for the overall system because it is no longer irreducible. In particular, this happens when $\epsilon = 0$ and $R_0 = G_{12}G_{21}$ or $G_{34}G_{43}$, and when $\epsilon = 1$ and $R_0 = G_{14}G_{41}$ or $G_{32}G_{23}$.

However, when $0 < \epsilon < 1$, the overall system has only one R_0, and (15) implies that R_0 is a continuously differentiable function in ϵ; hence, the sensitivity of R_0 to ϵ can be calculated by differentiating (15) with respect to ϵ to obtain $\partial R_0/\partial\epsilon$. An analytical calculation of $\partial R_0/\partial\epsilon$ when ϵ is close to 0 and 1 is provided in Appendix F.

Mathematically, when ϵ is not close to 0 or 1, it is difficult to analyze the rate of change of R_0 with respect to ϵ from (15). Next, We use two examples to understand how the connectivity strength ϵ affects R_0. We assume that in both upstream and downstream, one patch has better living condition (population has higher vital rates) than another one. The relation between R_0 and ϵ is plotted in Fig. 6.

As shown in Fig. 6, when $\epsilon = 0$ or $\epsilon = 1$ (i.e., there is no migration through straying routes), the subpopulation that migrate between two high quality patches has maximum net reproductive rate, denoted by $R_0^{\max}$, and the subpopulation

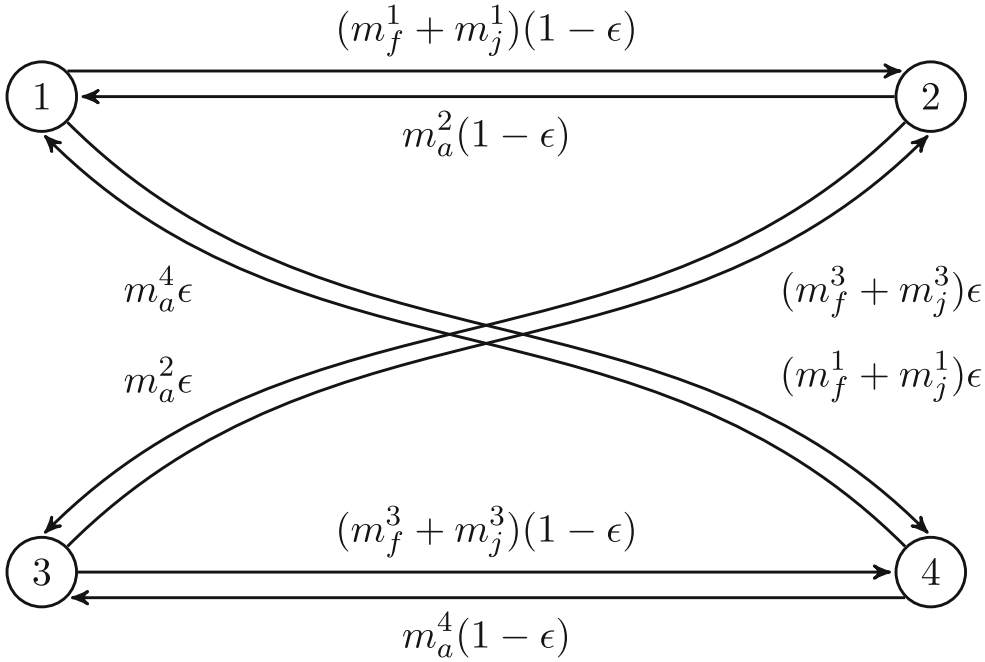

Fig. 5 Connectivity strength ϵ is realized by migration rates. Here m_a^2 represents the proportion that adults emigrate from the patch 2 to upstream for reproduction, that is, $m_a^2 = m_a^{12} + m_a^{32}$, here $m_a^{12} = m_a^2(1-\epsilon)$ and $m_a^{32} = m_a^2\epsilon$. Similar notations are applied to other migration rates

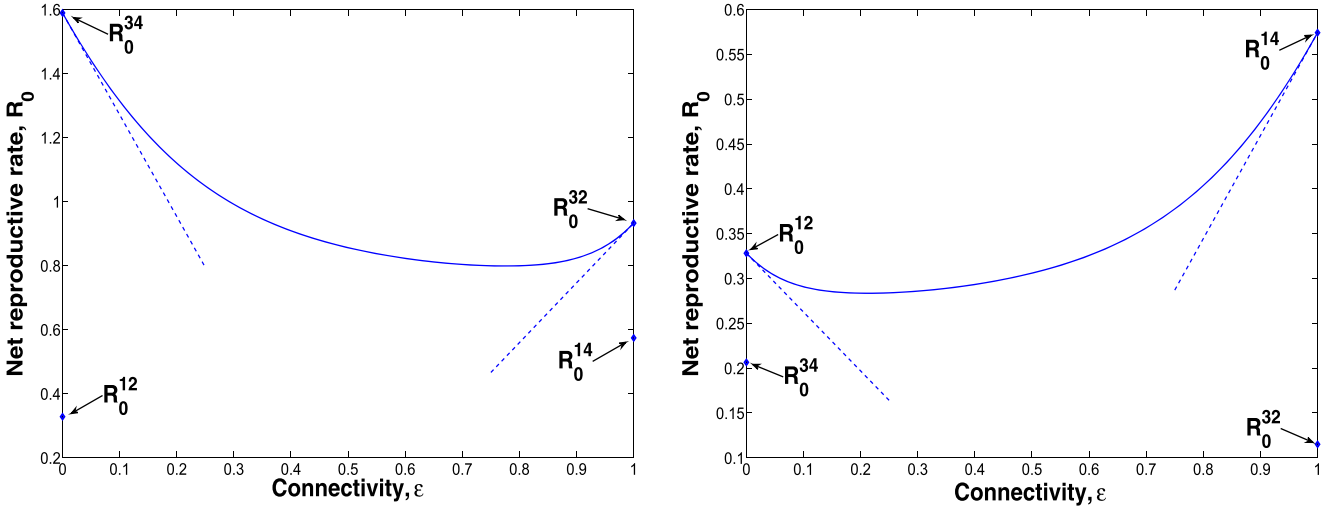

Fig. 6 The relation between the R_0 and the connectivity strength ϵ. *(Left)* Patch 3 is better than patch 1, patch 4 is better than patch 2. $b_1 = 500, m_a^2 = 0.3, m_f^1 = 0.4, m_j^1 = 0.6, p_{fe}^1 = 0.15, p_{jf}^1 = 0.1, p_{jj}^1 = 0.12, p_{jj}^2 = 0.15, p_{aj}^2 = 0.18, p_{aa}^2 = 0.2, p_{jf}^{21} = 0.125, p_{jj}^{21} = 0.135, b_3 = 750, m_f^3 = 0.6, m_j^3 = 0.9, p_{fe}^3 = 0.23, p_{jf}^3 = 0.15, p_{jj}^3 = 0.18, p_{jj}^4 = 0.195, p_{aj}^4 = 0.234, p_{aa}^4 = 0.26, p_{jf}^{23} = 0.15, p_{jj}^{23} = 0.18, p_{jf}^{43} = 0.17, p_{jj}^{43} = 0.19$. *(Right)* Patch 1 is better than patch 3, patch 4 is better than patch 2. $b_3 = 330, p_{fe}^3 = 0.1, m_f^3 = 0.3, m_j^3 = 0.4, p_{jf}^3 = 0.07, p_{jj}^3 = 0.08, p_{jf}^{23} = 0.11, p_{jj}^{23} = 0.12, p_{jf}^{43} = 0.13, p_{jj}^{43} = 0.14$. Other parameters are the same as in the left panel

that migrate between two poor quality patches has minimum net reproductive rate, denoted by $R_0^{\min}$. In particular, the left panel of Fig. 6 indicates that $R_0^{\max} = R_0^{34}$, $R_0^{\min} = R_0^{12}$, the right panel of Fig. 6 shows that $R_0^{\max} = R_0^{14}$, $R_0^{\min} = R_0^{32}$. As shown by the dashed lines in the Fig. 6, the slopes of the curves are negative when ϵ is close to 0, the slopes of the curves are positive when ϵ is close to 1 (see Eqs. 29–32 in the Appendix F for corresponding analytical results). Moreover, the left panel indicates that R_0 is less than but close to $R_0^{\max}$ when ϵ is close to 0, the right panel shows that R_0 is less than but close to $R_0^{\max}$ when ϵ is close to 1. These two examples imply that the overall population has a high net reproductive rate if most migrations (homing routes) occur between high quality patches or between poor quality patches, and very few migrations (straying routes) take place between high quality patches and poor quality patches. Hence, the high quality patches can be considered as "sources" and poor quality patches as "sinks." R_0 is largest when the sources are isolated from the sinks.

To further understand the relation between R_0 and connectivity strength ϵ, we assume that every patch has high or poor quality randomly, more precisely, we assume that the probability that each patch has high (poor) quality is 0.5 (0.5). We make Monte Carlo simulations by running 2000 samples. The relation between the mean of the net reproductive rates from 2000 samples and ϵ is plotted in Fig. 7. Figure 7 indicates again that a high R_0 value occurs when most of the population homes with great fidelity while the remaining ones stray.

The effect of homing fidelity on transient population persistence

The study on the effect of homing fidelity on net reproductive rate R_0 in the previous section concentrates on the asymptotic dynamics of the interacting model (12). The purpose of this section is to investigate the impact of homing fidelity, determined by connectivity strength ϵ, on transient growth rates based on the interacting model (12). By numerically solving the interacting model (12), we first show that depending on different initial distributions and connectivity strengthes, the population exhibits very different

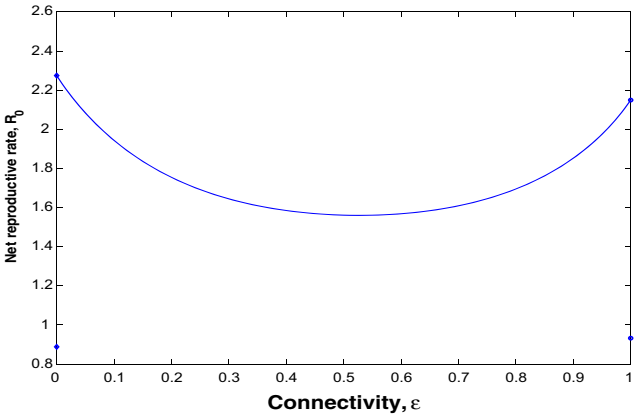

Fig. 7 The relation between the mean of net reproductive rates of 2000 realizations and the connectivity

transient growth rates that long-term results of R_0 analysis cannot reveal. This then motivate us to introduce two new measures, R_l and R_u, to predict the lowest and highest generational growth rates, respectively. Finally, we examine the effect of the migration behavior of subpopulations on R_l and R_u.

Transient behavior of interacting model

We consider a population whose dynamics is presented by the matrix model (1). According to Eq. 2, the net reproductive rate of the population, R_0, is given as the dominant eigenvalue of the next generation matrix $F(I-T)^{-1}$. Hence, there exists a dominant eigenvector $\xi > 0$ such that

$$F(I-T)^{-1}\xi = R_0\xi. \tag{16}$$

Under the constant conditions, the next generation population will ultimately grow at the rate R_0 and has the so-called stable structure (i.e., the distribution of abundance across stage, patch proportional to the eigenvector ξ). This implies that our previous discussion about the dependence of R_0 on connectivity strength ϵ assumes a stable population structure. The question arises as to what to expect if the population structure is not stable? In particular, we are interested in the following questions: (1) what is the short-term behavior of the system if the distribution of abundance across patch is variable? (2) How does homing fidelity affects short-term growth rate? To answer these questions, we solve the interacting model (12) using the same parameters as those in the left panel of Fig. 6. We compare the model solutions by choosing same connectivity strength ($\epsilon = 0.01$) but different initial distributions (all individuals as eggs in the poor quality patch and all individuals as eggs in the high quality patch) (left panel of Fig. 8). We also compare the model solutions by choosing same initial distribution (all individuals as eggs in the poor quality patch) but different connectivity strengthes ($\epsilon = 0.01$ and $\epsilon = 0.2$) (right panel of Fig. 8).

The left panel of Fig. 8 indicates that depending on different initial population structures, the transient solutions of the model are very different, even though their asymptotic behaviors are the same because of the same R_0 value. In fact, no matter what the initial distributions are, the population will eventually grow due to $R_0(0.01) > 1$ (left panel of Fig. 6).

The dependence of R_0 on ϵ (left panel of Fig. 6) shows that $R_0(0.01) > R_0(0.2) > 1$; hence in the long run, the population will eventually grow for both values of ϵ, and the next generation population will grow faster when $\epsilon = 0.01$ than it will when $\epsilon = 0.2$. However, as shown in the right panel of Fig. 8, with the initial distribution of all individuals as eggs in the poor quality patch (patch 1), the total population size decreases dramatically for both values of ϵ, and it takes a long time to achieve exponential growth. The population level when $\epsilon = 0.01$ is lower than that when $\epsilon = 0.2$ for a long time.

Transient measures of generational population growth: R_l and R_u

As we see from Figs. 2 and 8, the transient behavior of system may last a long time before the asymptotic behavior is achieved, thus the transient dynamics may be at least as important as asymptotic dynamics. Most indices for

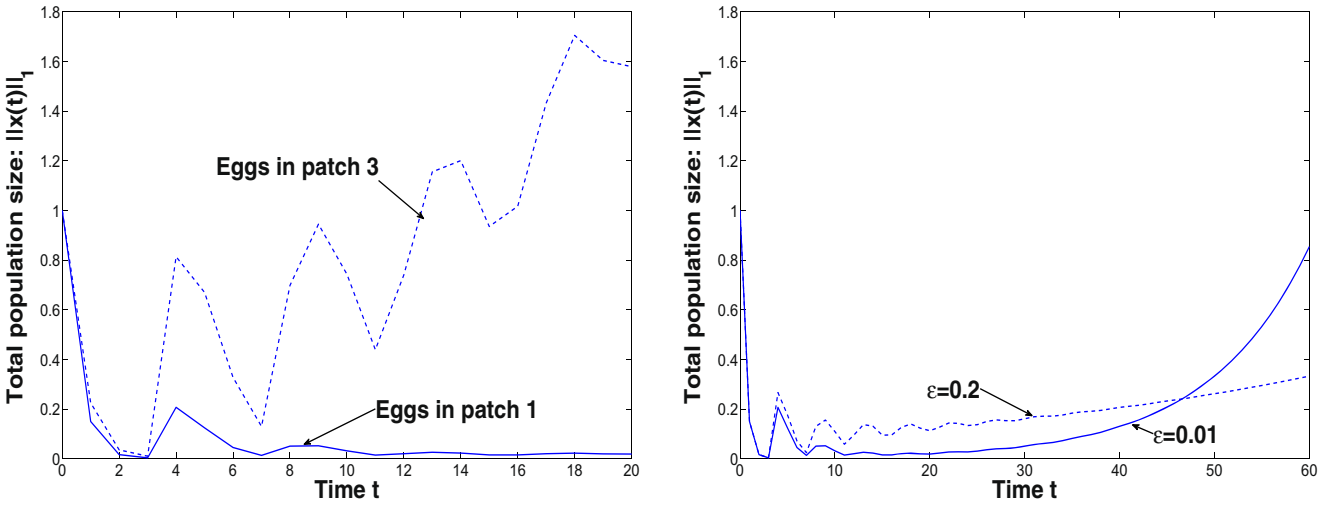

Fig. 8 (*Left*) Comparison of overall population size with same $\epsilon = 0.01$, but different initial population distribution: either $x(0)$=[1, 0, 0, 0, 0, 0, 0, 0, 0, 0]^T (*solid line*) or $x(0)$=[0, 0, 0, 1, 0, 0, 0, 0, 0, 0]^T (*dashed line*). (*Right*) Comparison of overall population size $||x(t)||_1$ with same initial population distribution $x(0)$=[1, 0, 0, 0, 0, 0, 0, 0, 0, 0]^T, but different connectivity strength ϵ: $\epsilon = 0.01$ (*solid line*), $\epsilon = 0.2$ (*dashed line*). The solid lines in both panels show the same trajectory but over different time scales

quantifying transient behavior, such as reactivity (10), λ_l (6), and λ_u (8) are too immediate to adequately describe transient behavior of the system. To avoid the "instantaneous" or "one time step" weakness of such indices, here we introduce two new measures, R_l and R_u, related to the next generation matrix, to describe intergenerational transient behavior. Noticing that most next generation matrices are degenerate, we define R_l and R_u based on the dominant submatrices of the next generation matrices, rather than next generation matrices themselves.

For convenience, we denote the next generation matrix $\mathbf{F}(\mathbf{I}-\mathbf{T})^{-1}$ by $\mathbf{Q}$. In the fecundity matrix $\mathbf{F}$, the (i, j) entry represents the expected number of i-class offsprings produced by a j-class individual per unit of time; in most matrix models, the number of offspring classes is less than the number of total classes, therefore, most fertility matrices are singular including zero rows. In those matrix models including only one newborn class, $\mathbf{F}$ has only one nonzero row, say the first row, consequently only the first row of $\mathbf{Q}$ is nonzero. This means, in this case, that $\mathbf{Q}$ has 0 as an $n-1$ repeated eigenvalues, and one dominant eigenvalue (net reproductive rate R_0) is the first row, first column entry.

More generally, suppose that there are $j > 1$ newborn classes. Without loss of generality, we list first j rows so that the last $n-j$ rows of $\mathbf{F}$ consist of zeros. If we denote the ith row of $\mathbf{F}$ by $\mathbf{F}_i$ and jth column of $(\mathbf{I}-\mathbf{T})^{-1}$ by τ_j, i.e.,

$$\mathbf{F} = \begin{pmatrix} \mathbf{F}_1 \\ \vdots \\ \mathbf{F}_j \\ \vdots \\ \mathbf{F}_n \end{pmatrix}, \qquad (\mathbf{I}-\mathbf{T})^{-1} = (\tau_1, \cdots, \tau_n),$$

then

$$\mathbf{Q} = \begin{pmatrix} \mathbf{F}_1\tau_1 & \cdots & \mathbf{F}_1\tau_j & \mathbf{F}_1\tau_{j+1} & \cdots & \mathbf{F}_1\tau_n \\ \vdots & \ddots & \vdots & \vdots & \ddots & \vdots \\ \mathbf{F}_j\tau_1 & \cdots & \mathbf{F}_j\tau_j & \mathbf{F}_j\tau_{j+1} & \cdots & \mathbf{F}_j\tau_n \\ 0 & \cdots & 0 & 0 & \cdots & 0 \\ \vdots & \ddots & \vdots & \vdots & \ddots & \vdots \\ 0 & \cdots & 0 & 0 & \cdots & 0 \end{pmatrix}.$$

Thus, the dominant eigenvalue of $\mathbf{Q}$ (net reproductive rate R_0) is the dominant eigenvalue of the submatrix from the upper left-hand corner, we denote it by $\mathbf{Q}_s$.

We define

$$R_l = \text{the minimum sum of column vectors of the matrix } \mathbf{Q}_s, \tag{17}$$

and

$$R_u = \text{the maximum sum of column vectors of the matrix } \mathbf{Q}_s. \tag{18}$$

Then, we have

$$R_l \le R_0 \le R_u. \tag{19}$$

Note that if the fecundity matrix $\mathbf{F}$ has only one nonzero row, say the first row, then $\mathbf{Q}_s$ degenerates into a one by one matrix with element $\mathbf{F}_1\tau_1$, in this case, $R_l = R_0 = R_u = \mathbf{F}_1\tau_1$.

Similarly as in the definition of λ_l (6) and λ_u (8), next we link the above definitions of R_l (17) and R_u (18) to minimum value and maximum value of the set $\{||\mathbf{Q}x||_1 : x \ge 0, ||x||_1 = 1\}$, respectively. For any $x = [x_1, \cdots, x_n]^T$, $\mathbf{Q}x = [y_1, \cdots, y_j, 0, \cdots, 0]^T$, where $y_k = \mathbf{F}_k\tau_1x_1 + \cdots + \mathbf{F}_k\tau_nx_n$, $k = 1, \cdots, j$. Hence, as an operator, the range of the next generation matrix $\mathbf{Q}$, denoted by $\mathrm{Ran}(\mathbf{Q})$, is the set of n-dimensional vectors with the last $n-j$ elements zero. We observe that

$$R_l = \min_{x\in\mathbb{R}^j, x\ge 0, ||x||_1=1} ||\mathbf{Q}_s x||_1 = \min_{x\in \mathrm{Ran}(\mathbf{Q}), x\ge 0, ||x||_1=1} ||\mathbf{Q}x||_1, \tag{20}$$

the minimum generational growth rate when initial population distributions belong to $\mathrm{Ran}(\mathbf{Q})$,

$$R_u = \max_{x\in\mathbb{R}^j, x\ge 0, ||x||_1=1} ||\mathbf{Q}_s x||_1 = \max_{x\in \mathrm{Ran}(\mathbf{Q}), x\ge 0, ||x||_1=1} ||\mathbf{Q}x||_1, \tag{21}$$

the maximum generational growth rate when initial population distributions belong to $\mathrm{Ran}(\mathbf{Q})$. Thus, R_l and R_u can be understood in terms of the worst or the best possible initial conditions for intergenerational growth. In particular, R_l can be thought of as the intergenerational growth rate under the worst possible initial conditions, and R_u can be thought of as the intergenerational growth rate under the best possible initial conditions.

Unlike λ_l and λ_u applying the project matrix to arbitrary nonnegative vectors in $\mathbb{R}^n$, R_l and R_u apply the next generation matrix to arbitrary nonnegative vector in $\mathrm{Ran}(\mathbf{Q})$. More strict discussion about this is provided in Appendix G.

Application to interacting model

We now study the effect of homing fidelity on transient population growth rates measured by R_l and R_u based on the interacting model (12). The fecundity matrix in model (12), denoted by $(f_{i,j})$, is a ten by ten matrix with only four nonzero elements: $f_{1,8} = b_1m_a^{1,2}$, $f_{1,10} = b_1m_a^{1,4}$, $f_{4,8} = b_3m_a^{3,2}$, and $f_{4,10} = b_3m_a^{3,4}$. Thus, the corresponding next generation matrix, denoted by $\mathbf{Q} := (q_{ij})$, is a ten by ten singular matrix with nonzero elements in the first and fourth rows, and zero elements in other rows. The associated dominant submatrix $\mathbf{Q}_s$ is then given by

$$\mathbf{Q}_s = \begin{pmatrix} q_{11} & q_{14} \\ q_{41} & q_{44} \end{pmatrix}.$$

Therefore,

$$R_l = \min\{q_{11} + q_{41}, q_{14} + q_{44}\}, \tag{22}$$

and

$$R_u = \max\{q_{11} + q_{41}, q_{14} + q_{44}\}. \tag{23}$$

Furthermore, following the proof of Eq. 6 (Appendix B), we can regard R_l as the intergenerational growth rate when all individuals as eggs initially distributed in the poor quality patch (say patch 1), that is $||\mathbf{Q}x||_1 = R_l$ when $x = [1, 0, 0, 0, 0, 0, 0, 0, 0, 0]^T$. Similarly, the generational growth rate is R_u if all individuals as eggs are initially distributed in the good quality patch.

Following Fig. 5, both R_l and R_u are functions in connectivity strength ϵ. As an example, we use the same parameters as those in Fig. 6 and choose $\epsilon \in [0, 1]$ to calculate $R_l(\epsilon)$ and $R_u(\epsilon)$. The graph of functions $R_0(\epsilon)$, $R_l(\epsilon)$, and $R_u(\epsilon)$ are compared in Fig. 9. When $\epsilon = 0$, the overall population is divided into two disjoint subpopulations (Fig. 5), and the four patch model reduces to two-disjoint two-patch models. Noticing that the fecundity matrix for each two-patch model has only one nonzero element, we have $R_l^{1,2} = R_0^{1,2} = R_u^{1,2}$ and $R_l^{3,4} = R_0^{3,4} = R_u^{3,4}$. Similarly, when $\epsilon = 1$, $R_l^{3,2} = R_0^{3,2} = R_u^{3,2}$ and $R_l^{1,4} = R_0^{1,4} = R_u^{1,4}$.

When $0 < \epsilon < 1$, as shown in the Fig. 9, the connectivity strength ϵ affects R_0 and R_u in similar way, but R_l in different way. To reduce the danger of population extinction in a generation, evaluated by the lowest generation growth rate R_l, one needs to choose ϵ which is not close 0 or 1 so as to maximize $R_l(\epsilon)$, even though R_0 reaches low values when ϵ is not close to 0 or 1. In other words, strong homing fidelity can increase the extinction hazard of endangered migratory salmonids in a single generation, even while increasing R_0 and R_u.

Discussion

Most models of population dynamics assume that species' resource are homogeneous in space (Fahrig and Merriam 1985). This assumption is often made in order to simplify mathematical analysis. However, spatial heterogeneity is one of the most obvious features of the natural world and is a key factor influencing population dynamics (Kareiva 1990). Populations experience spatial variation in environmental factors (e.g., temperature, precipitation, resource availability, and predation risk) which influence survivorship and reproduction, individuals can modulate their fitness (i.e., the net reproductive rate) by dispersing or migrating across space. Hence, interactions between movement and spatial heterogeneities determine how quickly a population grows or declines (Schreiber 2010). Understanding the interplay between connectivity (dispersal and migration) and local population dynamics allows persistence in a network of heterogeneous space is a central issue in population biology and has received increasing attention from theoretical, empirical and applied perspectives (Allen 1987; Gadgil 1971; Hamilton and May 1977; Hastings and Botsford 2006; Horn and Macarthur 1972; Kareiva 1990; Levin et al. 1984; Rieman and Dunham 2009; Schreiber 2010; Thomas and Kunin 1999; Vance 1984).

Research on the persistence of spatially structured populations has produced both theoretical and empirical evidence for a range of possible types of populations through various types of interacting systems of subpopulations (Hanski and Gilpin 1997; Thomas and Kunin 1999). Such population systems have generally been divided into discrete categories; for example, populations may be deemed to be "sources" or "sinks" (Pulliam 1988). As an important factor affecting population dynamics, demographic connectivity (dispersal and migration) among subpopulation's

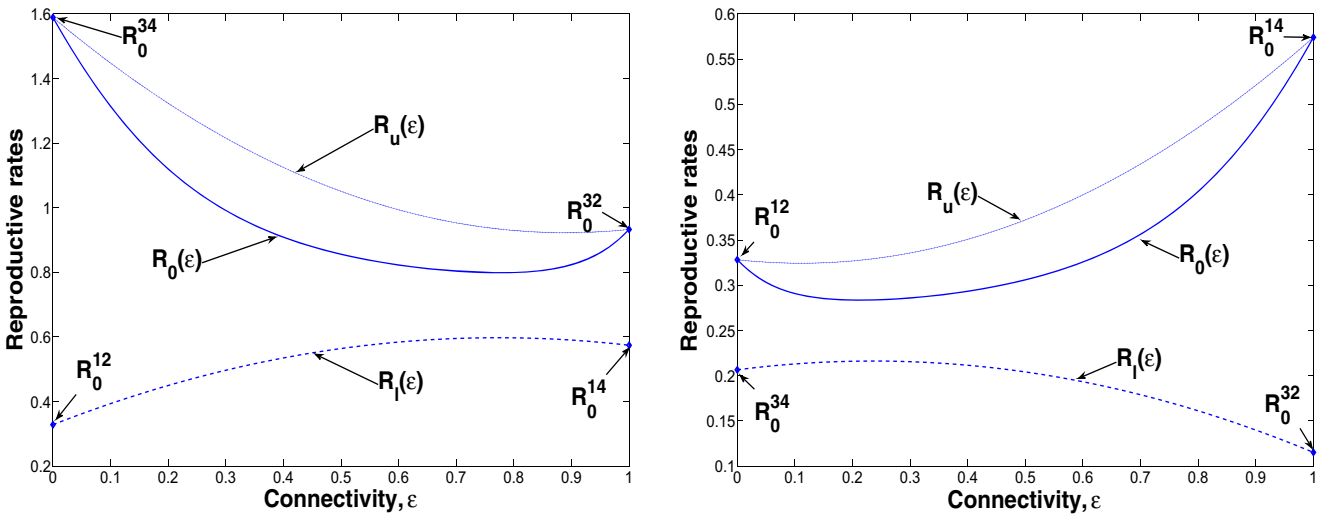

Fig. 9 Comparison of the graphs of functions $R_0(\epsilon)$, $R_l(\epsilon)$, and $R_u(\epsilon)$. We use the same parameters as those in Fig. 6

can contribute significantly to population growth rates, and ultimately population persistence. Therefore, assessing the effects of demographic connectivity on population persistence is crucial for understanding population biology and evolution in natural systems.

The main question we address in this paper is how the migration of individuals between spatially discrete habitats affects the long-run and short-run reproductive rates of migratory populations. We choose salmonidae as our study focus. Based on the life cycle of salmonds, we develop resident and migratory population models and extend the migratory population model to an interacting model. Unlike most stage-structured interacting models where population can complete its life cycle in each habitat, in the models for migratory salmonid, each habitat only supports part of stages.

With the underlying assumption that external conditions remain stable for long enough for the long-term dynamics to be reached, the results of asymptotic analysis about the dependence of R_0 on connectivity strength ϵ provide useful insights into the dynamics of interacting populations. In practice, when populations live in a stable or rather narrow range of predictable environment, we are likely to be concerned with their asymptotic long-term reproductive rate, measured by R_0. However, when populations confront environmental change and stochastic disturbance, their dynamics may never settle to behavior predicted by model asymptotics. Instead, populations can show transient growth or decay. In this case, R_0 is unable to predict the short-term transient dynamics that can arise. If we consider a endangered, threatened species, we should use R_l to assess the risk of extinction. If $R_l < 1$ and we introduce N_0 individuals, then it is possible that after a single generation we will have $R_l N_0$ individuals remaining. If this number falls below an extinction threshold, we could have population extinction even if $R_0 > 1$. On the other hand, R_u would be more applicable when assessing the threat posed by invasive species. Therefore, the long-term measure R_0 and short-term measures R_l and R_u are complementary, giving a range of valuable information for population conservation and management.

In the salmonidae example, we have studied the effect of migration behavior on the reproductive rate based on a four-patch model, where two patches are located in upstream and other two patches are located in downstream. However, in consideration of the fact that more than two streams might be located in upstream or downstream, one may want to construct a more complex multiple-patch model (Appendix H).

It is worth pointing out that, as with the four-patch model, multiple-patch model (33) assumes there is no population dispersing directly between upstream patches or directly between downstream patches. Therefore, two upstream patches do not interact with each other directly, but only indirectly through the migration which take place between downstream and upstream.

In the analysis, we use the same connectivity strength ϵ to evaluate the interactions between different four patches (Fig. 5). In reality, different connectivity strengthes may be related to different migration paths. An investigation on the effect of different connectivity strengths relevant to the different migration paths on R_0 is challenging and is left for future work.

We believe that the approach used in this paper is applicable in general to other migratory species. It is our hope that the conclusion about the effect of migration behaviors on population persistence will provide an insight to further understand the dynamics of migratory population. In addition, we hope to encourage the connection of data to these models in order to further understand their potential as management tools for assessing persistence of migratory populations under varying living conditions.

Acknowledgments

The authors wish to thank Alex Potapov, Andrew Paul, P. van den Driessche, and Lewis Lab for fruitful discussions. Q.H. gratefully acknowledges support from the Alberta Environment and Sustainable Resource Development and the Alberta Water Research Institute. M.A.L. also gratefully acknowledges a Canada Research Chair, NSERC Discovery and Accelerator grants, and a Killam Research Fellowship.

Appendix A: Graph reduction method

This method starts with the description of the projection matrix as a life cycle graph. Once the life cycle graph has been specified, the calculation procedure is as follows. (1) Identify survivorship and fecundity transitions. (2) Multiply all fecundity transitions in the graph by R_0^{-1}.(3) Eliminate survivorship self-loops, using rule **a** in Fig. 10. (4) Reduce the graph using the graph reduction rules defined in Figure I until only nodes with fecundity self-loops are left. When a node is eliminated, all pathways that go through that node have to be recalculated. (5) If only one node with a single self-loop is left, eliminate the final node by setting the self-loop equal to 1 and solve this equation for R_0.

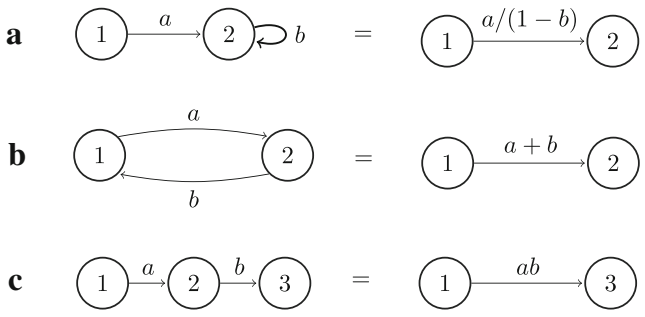

Fig. 10 Graph reduction rules. **a** self-loop elimination with $b < 1$. **b** Parallel path elimation. **c** Node elimination. Rules **a** and **b** show elimination of paths, and rule **c** shows the elimination of node 2. Graph reduction is done by repeatedly applying these rules until only nodes are left

Appendix B: Proof of (6)

To investigate the function $\mathbf{P}x$, we let $\mathbf{P} = (p_{ij})_{n\times n}$ and $x = [x_1, x_2, \cdots, x_n]^T$. A simple calculation gives

$$||\mathbf{P}x||_1 = \sum_{i=1}^{n} p_{i1}x_1 + \sum_{i=1}^{n} p_{i2}x_2 + \cdots + \sum_{i=1}^{n} p_{in}x_n, \quad (24)$$

Noticing that $\sum_{i=1}^{n} p_{ij} (j = 1, \cdots, n)$ is the j^{th} column sum of the matrix $\mathbf{P}$, we consider the smallest such column sum of $\mathbf{P}$. Suppose that for some $1 \le k \le n$, $\sum_{i=1}^{n} p_{ik} = \min_{1\le j\le n} \sum_{i=1}^{n} p_{ij}$, then the function $||\mathbf{P}x||_1$ has minimum value $\sum_{i=1}^{n} p_{ik}$ when x is a unit vector with $x_k = 1$ and $x_j = 0$ $(j \ne k)$. That is to say,

$$\lambda_l = \min_{1\le j\le n} \sum_{i=1}^{n} p_{ij}, \quad (25)$$

the minimum sum of column vectors of projection matrix $\mathbf{P}$.

Appendix C: R_0 for resident salmonids

In terms of the life cycle of resident species, we divide the population into four groups: fertilized egg (E), fry (F), juvenile (J), and adult (A). We take time unit to be 1 year. The population vector is $x(t) = [E(t), F(t), J(t), A(t)]^T$, which represents the population density of each stage at the end of the breeding season in year t. We relate the population density of each stage at time $t+1$ to time t by the matrix equation

$$x(t + 1) = \mathbf{P}x(t), \quad (26)$$

where the projection matrix $\mathbf{P}$ is

$$\mathbf{P} = \begin{pmatrix} 0 & 0 & 0 & b \\ p_{fe} & 0 & 0 & 0 \\ 0 & p_{jf} & p_{jj} & 0 \\ 0 & 0 & p_{aj} & p_{aa} \end{pmatrix}.$$

Here, b is the average number of fertilized eggs produced per adult per year, p_{fe} is the proportion of eggs that hatch to fry stage each year, p_{jf} is the proportion of fry that survive to the juvenile stage each year, p_{jj} is the proportion of juveniles that survive to remain as a juvenile per year, p_{aj} is the proportion of juveniles that survive to become adults each year, p_{aa} is the proportion of adults that survive each year. The vital rates of salmonids living a variety of environment have been estimated by many researchers (e.g., (Al-Chokhachy and Budy 2008; Bowerman and Budy 2012; McPhail and Baxter 1996)).

The matrix Eq. 26 models the dynamics of resident salmonids population. The net reproductive rate, R_0, for this population can be calculated using the graph reduction method, as mentioned in Appendix A. The graph reduction method is shown in Fig. 11.

From the equation of R_0 (Fig. 11d), we see that the proportion of individuals that start as eggs and eventually mature and survive to become breeding adults is $p_{fe}p_{jf}$ $p_{aj}/[(1 - p_{jj})(1 - p_{aa})]$, and the expected number of eggs produced per breeding adult is b. Multiplying these quantities yields R_0.

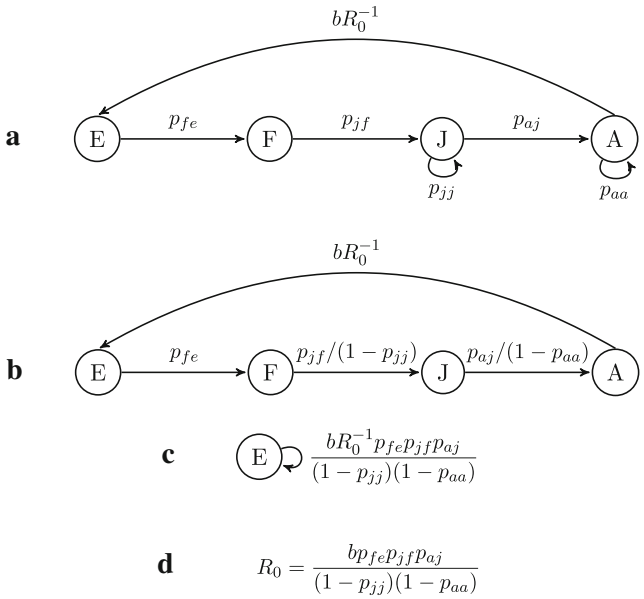

Fig. 11 **a** The full transformed graph. **b** Eliminating self-loops. **c** Eliminating nodes F, J, and A. **d** Solving for R_0

Appendix D

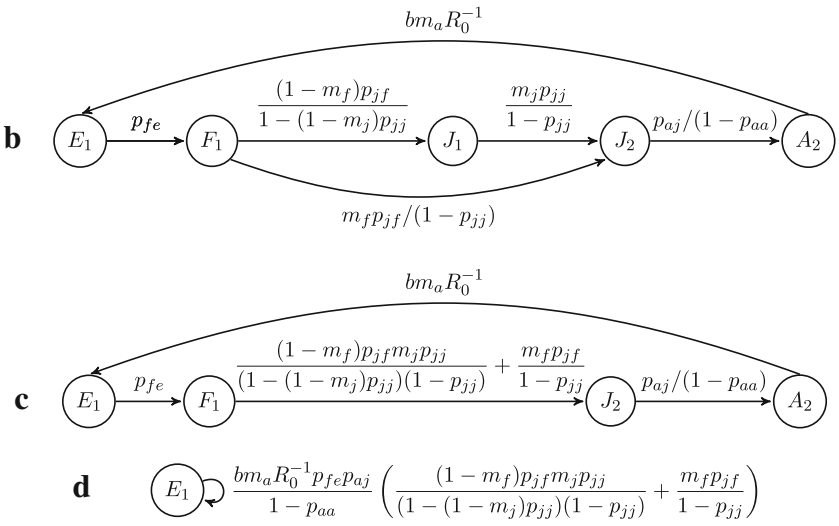

Appendix E

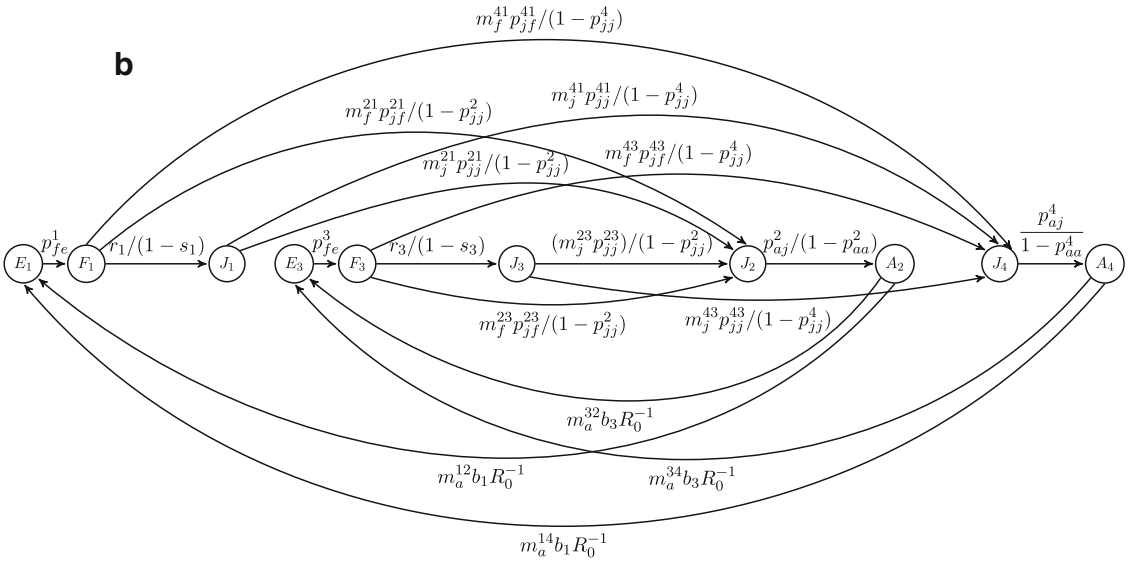

$$r_1=(1-m_f^{21}-m_f^{41})p_{jf}^1,\quad s_1=(1-m_j^{21}-m_j^{41})p_{jj}^1,\quad r_3=(1-m_f^{23}-m_f^{43})p_{jf}^3,\quad s_3=(1-m_j^{23}-m_j^{43})p_{jj}^3$$

Fig. 12 **b** Eliminating self-loops. **c** Eliminating node J_1. **d** Eliminating nodes F_1, J_2, and A_2

Fig. 13 **b** Eliminating self-loops. **c** Eliminating nodes E_1, E_3, A_2 and A_4. **d** Eliminating nodes J_1 and J_3. **e** Eliminating nodes J_2 and J_4. **f** Eliminating nodes F_3

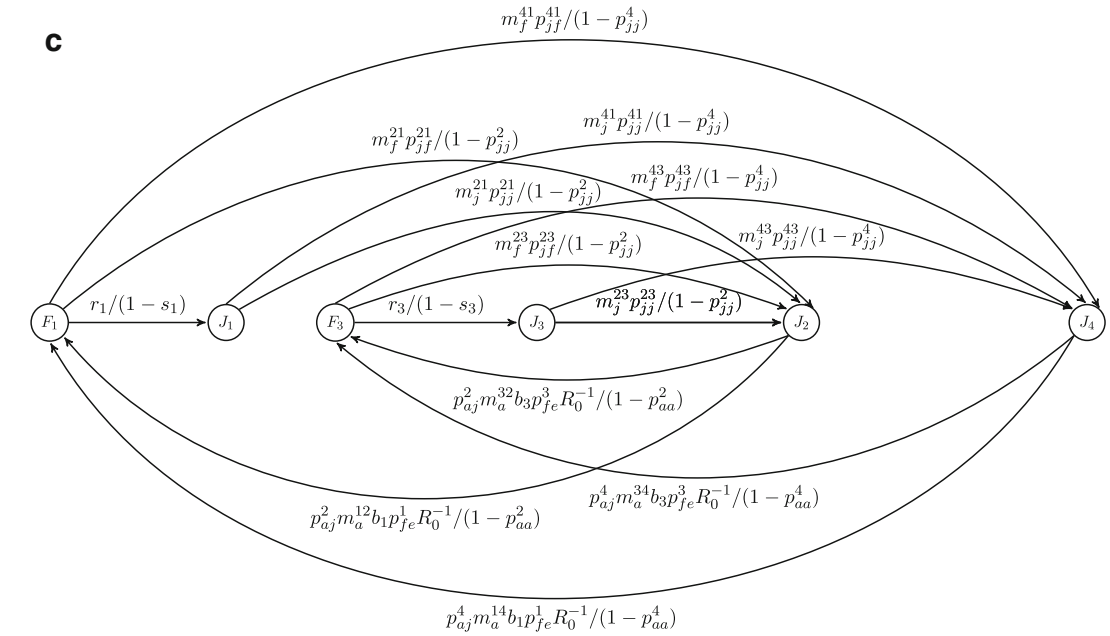

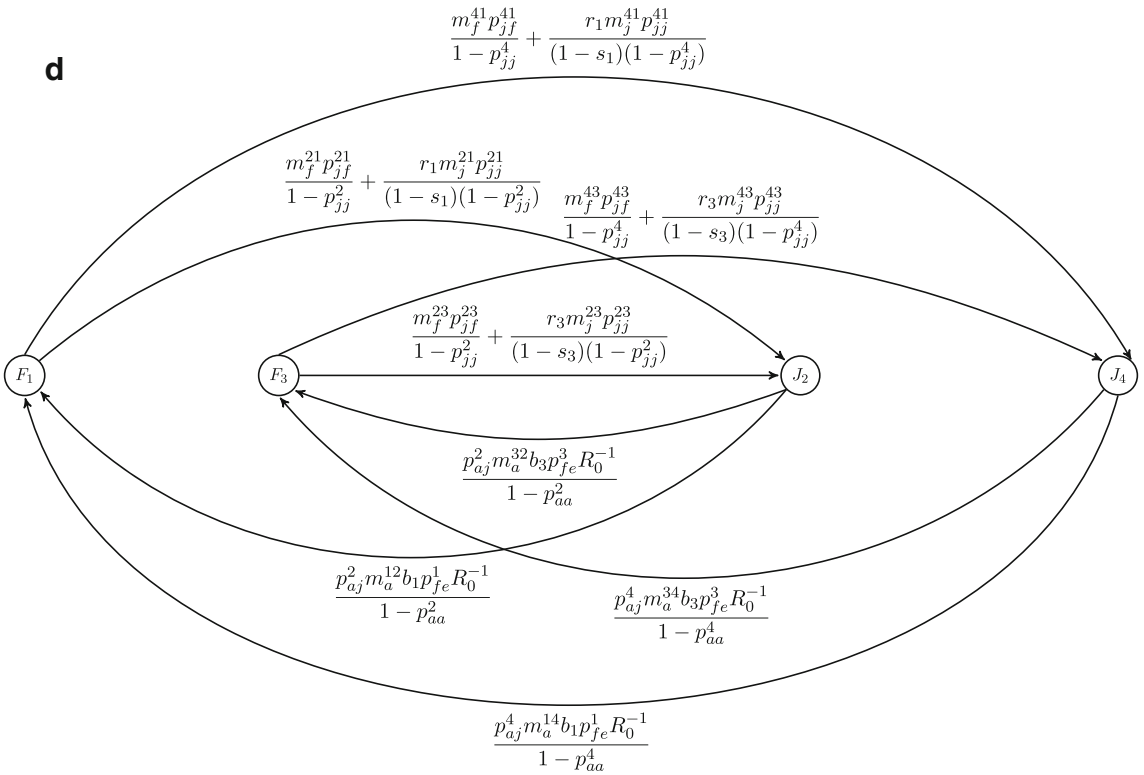

Fig. 13 (continued)

Fig. 13 (continued)

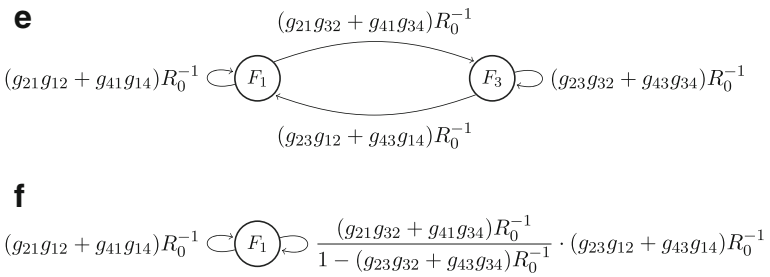

Appendix F: An analytical calculation of $\partial R/\partial\epsilon$ when ϵ is close to 0 and 1

We differentiate the Eq. 15 with respect to ϵ to get

$$2R_0\frac{\partial R_0}{\partial\epsilon}+[2A(1-\epsilon)-2B\epsilon]R_0-\left[A(1-\epsilon)^2+B\epsilon^2\right]\frac{\partial R_0}{\partial\epsilon}$$
$$-C\left(2\epsilon-6\epsilon^2+4\epsilon^3\right)+4D\epsilon^3-4E(1-\epsilon)^3=0.$$

Thus,

$$\frac{\partial R_0}{\partial\epsilon}=\frac{2AR_0(\epsilon-1)+2BR_0\epsilon+C\left(2\epsilon-6\epsilon^2+4\epsilon^3\right)-4D\epsilon^3+4E(1-\epsilon)^3}{2R_0-A(1-\epsilon)^2-B\epsilon^2}. \tag{27}$$

Hence,

$$\lim_{\epsilon\to0^+}\frac{\partial R_0}{\partial\epsilon}=\frac{-2AR_0\left(0^+\right)+4E}{2R_0(0^+)-A}. \tag{28}$$

Noticing that $R_0(0^+)=\max\{G_{21}G_{12},G_{43}G_{34}\}$, we find

$$\begin{aligned}\lim_{\epsilon\to0^+}\frac{\partial R_0}{\partial\epsilon}&=\frac{-2(G_{21}G_{12}+G_{43}G_{34})\max\{G_{21}G_{12},G_{43}G_{34}\}+4G_{21}G_{12}G_{43}G_{34}}{2\max\{G_{21}G_{12},G_{43}G_{34}\}-G_{21}G_{12}-G_{43}G_{34}}\\&=-2\max\{G_{21}G_{12},G_{43}G_{34}\}.\end{aligned} \tag{29}$$

Since $R_0(1^-)=\max\{G_{23}G_{32},G_{41}G_{14}\}$, similar computation yields

$$\lim_{\epsilon\to1^-}\frac{\partial R_0}{\partial\epsilon}=2\max\{G_{23}G_{32},G_{41}G_{14}\}. \tag{30}$$

If $0<\epsilon\ll1$, the function $R_0(\epsilon)$ can be approximated by a straight line

$$\begin{aligned}R_0(\epsilon)&\approx R_0\left(0^+\right)+\left(\lim_{\epsilon\to0^+}\frac{\partial R_0}{\partial\epsilon}\right)\epsilon\\&=\max\{G_{21}G_{12},G_{43}G_{34}\}\\&\quad-2\max\{G_{21}G_{12},G_{43}G_{34}\}\epsilon,\end{aligned} \tag{31}$$

with negative slope.

Similarly, if ϵ is less than and sufficiently close to 1, then we have

$$\begin{aligned}R_0(\epsilon)&\approx R_0(1^-)+\left(\lim_{\epsilon\to1^-}\frac{\partial R_0}{\partial\epsilon}\right)(\epsilon-1)\\&=-\max\{G_{23}G_{32},G_{41}G_{14}\}\\&\quad+2\max\{G_{23}G_{32},G_{41}G_{14}\}\epsilon.\end{aligned} \tag{32}$$

with positive slope.

Appendix G: Further discussion about R_l and R_u

For the matrix $\mathbf{Q}$, we define the range of $\mathbf{Q}$ as $\mathrm{Ran}(\mathbf{Q})=\{\mathbf{Q}x|x\in\mathbb{R}^n\}$, and the null space of $\mathbf{Q}$ as $\mathcal{N}(\mathbf{Q})=\{x\in\mathbb{R}^n|\mathbf{Q}x=0\}$.

Then both $\mathrm{Ran}(\mathbf{Q})$ and $\mathcal{N}(\mathbf{Q})$ are subspaces of $\mathbb{R}^n$, and $\mathbb{R}^n=\mathrm{Ran}(\mathbf{Q})\bigoplus\mathcal{N}(\mathbf{Q})$. Therefore, for any $x\in\mathbb{R}^n$, there exists unique $x_{\mathrm{Ran}}\in\mathrm{Ran}(\mathbf{Q})$ and unique $x_{\mathcal{N}}$ such that $x=x_{\mathrm{Ran}}+x_{\mathcal{N}}$. Thus, for any $x\in\mathbb{R}^n$, $\mathbf{Q}x=\mathbf{Q}x_{\mathrm{Ran}}+\mathbf{Q}x_{\mathcal{N}}=\mathbf{Q}x_{\mathrm{Ran}}+0$. The projection of any $x\in x_{\mathcal{N}}$ will give zero individual in the next generation, which is not of biological interest. For this reason, we restrict $x\in\mathrm{Ran}(\mathbf{Q})$ when defining R_l and R_u.

Appendix H: A multiple-patch model

If we assume that there are I small rivers in upstream and K big rivers in downstream, it is not difficult to extend the four-patch model (12) to a multiple-patch model:

$$\begin{aligned}E_i(t+1)&=\sum_{k=1}^{K}b_i m_a^{ik}A_k(t)\\F_i(t+1)&=p_{fe}^{i}E_i(t)\\J_i(t+1)&=\left(1-\sum_{k=1}^{K}m_f^{ki}\right)p_{jf}^{i}F_i(t)+\left(1-\sum_{k=1}^{K}m_j^{ki}\right)p_{jj}^{i}J_i(t)\\J_k(t+1)&=\sum_{i=1}^{I}\left(m_f^{ki}p_{jf}^{ki}F_i(t)+m_j^{ki}p_{jj}^{ki}J_i(t)\right)\\A_k(t+1)&=p_{aj}^{k}J_k(t)+p_{aa}^{k}A_k(t),\end{aligned} \tag{33}$$

for $i=1,2,\cdots,I$ and $k=1,2,\cdots,K$.

References

Al-Chokhachy R, Budy P (2008) Demographic characteristics, population structure, and vital rates of a fluvial population of bull trout in Oregon. Trans Am Fish Soc 137:262–277

Allen L (1987) Extinction and critical patch number for islands populations. J Math Biol 24:617–625

Berman A, Plemmons RJ (1994) Nonnegative matrices in the mathematical sciences, Society for Industrial and applied Mathematics, Philadelphia, Pennsylvania. U.S.A

Bowerman T, Budy P (2012) Incorporating movement patterns to improve survival estimates for juvenile bull trout. North Am J Fish Manag 32:1123–1136

de-Camino-Beck T, Lewis MA (2007) A new method for calculating net reproductive rate from graph reduction with application to the control of invasive species. Bull Math Biol 69:1341–1354

Caswell H (2001) Matrix Population Models. Sinauer Assosiate, Sunderland

Caswell H, Neubert MG (2005) Reactivity and transient dyanmics of discrete-time ecological systems. J Differ Equ Appl II 4-5:295–310

Cushing J, Zhou Y (1994) The net reproductive value and stability in matrix population models. Nat Resour Model 8:297–333

Deangelis DL, Post WM, Travis CC (1986) Positive Feedback In Natural Systems, vol 15. Springer-Verlag, New York

Ellner S (1984) Asymptotic behavior of some stochastic difference equation population models. J Math Biol 19:169–200

Ezard THG, Bullock JM, Dalgleish HJ, Million A, Pelletier F, Ozgul A, Koons DN (2010) Matrix models for a changeable world: the importance of transient dynamics in population management. J Appl Ecol 47:515–523

Fahrig L, Merriam G (1985) Habitat patch connectivity and population survival. Ecology 66:1762–1768

Fraley JJ, Shepard BB (1989) Life history, ecology and population status of migratory bull trout (Salvelinus confluentus) in the Flathead lake and river system, Montana. Northwest Sci 63:133–143

Gadgil M (1971) Dispersal: Population consequences and evolution. Ecology 52:253–261

Hamilton WD, May RM (1977) Dispersal in stable habitats. Nature 269:578–581

Hanski IA, Gilpin ME (1997) Metapopulation biology: Ecology, genetics, and evolution. Academic Press, San Diego, California

Hastings A (2001) Transient dynamics and persistence of ecological systems. Ecol Lett 4:215–220

Hastings A (2004) Transients: the key to long-term ecological understanding Trends Ecol Evol 19:39–45

Hastings A, Botsford L (2006) Persistence of spatial populations depends on returning home. Proc Nat Acad Sci USA 103:6067–6072

Horn HL, Macarthur RH (1972) Competition among fugitive species in harlequin environment. Ecology 53:749–752

Horn RA, Johnson CR (2013) Matrix Analysis. 2nd edition

Kareiva P (1990) Population dynamics in spatially comples environments: Theory and data. Phil Trans R Soc Lond B 330:175–190

Koons DN, Holmes RR, Grand JB (2007) Population inertia and its sensitivity to changes in vital rates and population structure. Ecology 88:2857–2867

Levin SA, Cohen D, Hastings A (1984) Dispersal stratgies in patch environment. Theor Popul Biol 26:165–191

Pulliam HR (1988) Source, sinks, and population regulation. Am Nat 132:652–661

Li C, Schneider H (2002) Applications of Perron-Frobenius theory to population dynamics. J Math Biol 44:450–462

Macarthur RH, Wilson EO (1967) The theory of island biogeography. Princeton University Press, Princeton, NJ

McPhail JD, Baxter JS (1996) A review of bull trout life-history and habitat use in relation to compensation and improvement opportunities, Fisheries Management Report No. 104

Neubert MG, Caswell H (1997) Alternatives to resilience for measuring the responses of eoclogical systems to perturbations. Ecology 78:653–665

Ortega JD (1987) Matrix Thory: A Second Course. Plenum Press, New York

Pacific Salmonids (2014) Major Threats and Impacts, NOAA fisheries office of protected resource, http://www.nmfs.noaa.gov/pr/species/fish/salmon.htm

Rieman BE, Dunham JB (2009) Metapopulations and salmonids: a synthesis of life history patterns and empirical observations. Ecol Freshwat Fish 9:51–64

Rogers A (1968) Matrix analysis of international population growth and distribution. University of California Press, Berkeley, California

Rogers A (1995) Multiregional demography: Principles, methods and extensions. Wiely, New York

Rueffler C, Metz JAJ (2013) Necessary and sufficient conditions for R_0 to be a sum of contributions of fertility loops. J Math Biol 66:1099–1122

Schreiber SJ (2010) Interactive effects of temporal correlations, spatial heterogeneity and dispersal on population persistence. Proc Royal Soc B 277:1907–1914

Stewart IJ, Carlson SM, Boatright CP, Buck GB, Quinn TP (2004) Site fidelity of spawning sockeye salmon (Oncorhynchus nerka W.) in the presence and absence of olfactory cues. Ecol Freshwat Fish 13:104–110

Stott I, Townley S, Hodgson DJ (2011) A framework for studying transient dynamics of population projection matrix models. Ecol Lett 14:959–970

Townley S, Carsilake D, Smith OK, Mccarthy D, Hodgson D (2007) Predicting transient amplification in perturbed ecological systems. J Appl Ecol 44:1243–1251

Thomas CD, Kunin WE (1999) The spatial structure of populations. J Anim Ecol 68:647–657

Underwood K, Cramer SP (2007) simulation of human effects on bull trout population dynamics in Rimrock Reservoir, Washington. Ametican Fish Soc 53:191–207

Vance RR (1984) The effect of dispersal on population stability in one-species, discrete-space population growth models. Am Nat 123:230–254

Salmonidae (2014) Animal diversity web, http://animaldiversity.ummz.umich.edu/accounts/Salmonidae/